

Drift Barriers to Quality Control When Genes Are Expressed at Different Levels

Kun Xiong,* Jay P. McEntee,[†] David J. Porfiro,[‡] and Joanna Masel^{*,1}

*Department of Molecular and Cellular Biology, [†]Department of Ecology & Evolutionary Biology, and [‡]Department of Computer Science, University of Arizona, Tucson, Arizona 85721

ORCID IDs: 0000-0003-1431-6586 (K.X.); 0000-0002-1213-9734 (J.P.M.); 0000-0001-5383-3266 (D.J.P.); 0000-0002-7398-2127 (J.M.)

ABSTRACT Gene expression is imperfect, sometimes leading to toxic products. Solutions take two forms: globally reducing error rates, or ensuring that the consequences of erroneous expression are relatively harmless. The latter is optimal, but because it must evolve independently at so many loci, it is subject to a stringent “drift barrier”—a limit to how weak the effects of a deleterious mutation s can be, while still being effectively purged by selection, expressed in terms of the population size N of an idealized population such that purging requires $s < -1/N$. In previous work, only large populations evolved the optimal local solution, small populations instead evolved globally low error rates, and intermediate populations were bistable, with either solution possible. Here, we take into consideration the fact that the effectiveness of purging varies among loci, because of variation in gene expression level, and variation in the intrinsic vulnerabilities of different gene products to error. The previously found dichotomy between the two kinds of solution breaks down, replaced by a gradual transition as a function of population size. In the extreme case of a small enough population, selection fails to maintain even the global solution against deleterious mutations, explaining the nonmonotonic relationship between effective population size and transcriptional error rate that was recently observed in experiments on *Escherichia coli*, *Caenorhabditis elegans*, and *Buchnera aphidicola*.

KEYWORDS cryptic genetic variation; stop codon readthrough; robustness; evolvability; transcriptional errors; proofreading

In classical population genetic models of idealized populations, the probability of fixation of a new mutant depends sharply on the product of the selection coefficient, s , and the population size, N . As s falls below $-1/N$, fixation probabilities drop exponentially, corresponding to efficient selective purging of deleterious mutations. For $s > -1/N$, random genetic drift makes the fate of new mutants less certain. This nonlinear dependence of fixation probability on sN has given rise to the “drift barrier” hypothesis (Lynch 2007), which holds that populations are characterized by a threshold or “barrier” value of the selection coefficient, s , corresponding to the tipping point at which the removal of deleterious mutations switches between effective and ineffective. In idealized populations, described by Wright-Fisher or Moran models, the

drift barrier is positioned at $s = \sim -1/N$. Drift barriers also exist, albeit sometimes with less abrupt threshold behavior, in more complex models of evolution in which some assumptions of an idealized population are relaxed (Good and Desai 2014).

The drift barrier theory argues that variation among species in their characteristic threshold values for s , thresholds that are equal by definition to the inverse of the selection effective population size, N_e , can explain why different species have different characteristics, e.g., streamlined vs. bloated genomes (Lynch 2007). The simplest interpretation of the drift barrier would seem to imply that large- N_e species show stricter quality control over all biological processes, e.g., higher fidelity in DNA replication, transcription, and translation, than small- N_e species, because molecular defects in quality control mechanisms are less effectively purged in the latter (Lynch 2010; Traverse and Ochman 2016a).

However, the data reveal more complex patterns. Unsurprisingly, *Buchnera aphidicola*, which has exceptionally low N_e (Mira and Moran 2002; Rispe *et al.* 2004), has a higher transcriptional error rate, at 4.67×10^{-5} (Traverse and Ochman 2016b), than the error rate 4.1×10^{-6} previously

Copyright © 2017 by the Genetics Society of America

doi: 10.1534/genetics.116.192567

Manuscript received June 11, 2016; accepted for publication November 2, 2016; published Early Online November 11, 2016.

Supplemental material is available online at www.genetics.org/lookup/suppl/doi:10.1534/genetics.116.192567/-/DC1.

¹Corresponding author: Department of Ecology and Evolutionary Biology, University of Arizona, 1041 E. Lowell St., Tucson, AZ 85721. E-mail: masel@email.arizona.edu

reported for *Caenorhabditis elegans* (Gout *et al.* 2013). But, to the surprise of the authors, the error rate in large- N_e *Escherichia coli* is highest of all, at 8.23×10^{-5} (Traverse and Ochman 2016b).

A more refined drift barrier theory can explain these findings. As the fitness burden accumulates from the slightly deleterious mutations that a small- N_e species cannot purge, some forms of quality control may evolve as a second line of defense. The ideal solution is to purge all deleterious mutations, even those of tiny effect; when this first line of defense fails, the second line of defense is to ameliorate the cumulative phenotypic consequences of the deleterious mutations that have accumulated (Frank 2007; Rajon and Masel 2011; Warnecke and Hurst 2011; Lynch 2012; Wu and Hurst 2015). The first line of defense bears no fitness cost (purging is free), but faces a stringent drift barrier; the second line of defense also solves the problem but at a cost. In some circumstances, as described further below, strict quality control can act as a second-line amelioration strategy (Rajon and Masel 2011). The existence of two distinct lines of defense complicates the naive drift barrier logic that large- N_e species should generally exhibit stricter quality control in all molecular processes. The superior performance of large- N_e species in a primary line of defense other than quality control may remove any advantage of strict and costly quality control as a secondary line of defense. This creates a seemingly counter-intuitive pattern in quality control, in which small- N_e species can evolve more faithful processes than large- N_e species such as *E. coli*.

The existence of two substantively different strategies was first proposed by Krakauer and Plotkin (2002), who contrasted “redundancy” (robustness to the consequences of mutational errors) with “antiredundancy” (hypersensitivity to mutations). By positing that the redundancy strategy is costly, they find that only small- N_e species suffer from a large enough drift load (Kimura *et al.* 1963) to make this cost, and hence redundancy, worthwhile. Large N_e species not burdened by drift load are able to adopt the alternative antiredundancy strategy, which bears no cost, and hence allows the population to achieve higher fitness.

A related argument was made by Rajon and Masel (2011) in the context of mitigating the harms threatened by errors in molecular processes such as translation. Rajon and Masel (2011) distinguished between “local” solutions, where a separate solution is required at each locus, and “global” solutions that can deal with problems at many loci simultaneously. The evolution of extensive quality control mechanisms was deemed a global solution because a single mutation impacting general quality control mechanisms can affect the prevention of gene expression errors at many loci. Note that quality control includes not only mechanisms such as proofreading for preventing errors from happening in the first place, but also mechanisms that reduce downstream damage from errors, *e.g.*, degradation of mRNA molecules that seem faulty. Global quality control should come with a cost in time or energy.

Rajon and Masel’s (2011) alternative, local solution is to have a benign rather than a strongly deleterious “cryptic

genetic sequence” at each locus at which expression errors might occur, making the consequence of an error at that locus relatively harmless. In contrast to the global solution, these local solutions bear no direct fitness cost, but because selection at any one locus is weak, they are more difficult to maintain than global solutions. The local solution corresponds to a low number of mutations, k , in Krakauer and Plotkin (2002).

Both the quality control of Rajon and Masel (2011) and the redundancy of Krakauer and Plotkin (2002) to the consequences of mutations are global across loci, and also costly. Meantime, both the local solutions of Rajon and Masel (2011) and the reduction in the number of mutations, k , that accompanies the antiredundancy of Krakauer and Plotkin (2002) carry no true fitness cost, but instead require a large- N_e drift barrier as a limit to their adaptation. A mutation disrupting a solution specific to a single locus requires a large value of N_e for its purging, whereas a mutation disrupting a global quality control mechanism will have large fitness consequences and so be easier to purge. As a consequence, only large N_e populations evolve the higher-fitness local solution, while it is the small N_e populations that evolve global solutions such as extensive (and costly) quality control.

Selection to achieve the local solution by purging deleterious mutations to cryptic sequences (leaving in place genotypes whose cryptic genetic sequences are benign) may be difficult and hence restricted to high- N_e populations. There are, however, reasons to believe that it is not impossible. For example, when the error in question is reading through a stop codon, the local cryptic genetic sequence is the 3’ UTR, which is read by the ribosome. One option for a more benign form of this cryptic sequence is the presence of a “backup” stop codon that provides the ribosome with a second and relatively early chance to terminate translation. Such backup stops are common at the first position past the stop in prokaryotes (Nichols 1970). In *Saccharomyces cerevisiae*, there is also an abundance of stop codons at the third codon position past the stop (Williams *et al.* 2004). Moreover, conservation at this position depends strongly on whether or not the codon is a stop, and the overrepresentation of stops at this position is greater in more highly expressed genes (Liang *et al.* 2005). In some ciliates, where the genetic code has been reassigned, so that UAA and UAG correspond to glutamine, this overrepresentation is much more pronounced (Adachi and Cavalcanti 2009). As with the consequences of erroneous readthrough, selective pressure on erroneous amino acid misincorporation and/or misfolding (Drummond and Wilke 2008), and on erroneous protein–protein interactions (Brettner and Masel 2012), are also strong enough to shape protein expression and interaction patterns. In the case of transcriptional errors, while both *E. coli* and *B. aphidicola* have high error rates, only *E. coli* shows signs of having evolved a first line of defense in the form of a decreased frequency, with which observed transcriptional errors translate into nonsynonymous changes relative to randomly sampled transcriptional errors (Traverse and Ochman 2016a).

Rajon and Masel (2011) found that, for intermediate values of N_e that correspond strikingly well to many multicellular species of interest, the evolutionary dynamics of the system were bistable, with either the global or the local solution possible. This is a natural consequence of a positive feedback loop; in the presence of a strict global quality control mechanism, specialized solutions at particular loci are unnecessary, and mutations destroying them pass through the drift barrier (we use the expression “pass through the drift barrier” to mean that $0 > s > -1/N$), with their subsequent absence increasing the demand for quality control. Similarly, when specialized solutions predominate, the advantage to quality control is lessened, and resulting higher error rates further increase selection for many locally specialized solutions. If true, this bistability suggests that historical contingency, rather than the current value of N_e , determines which processes are error-prone vs. high-fidelity for populations at intermediate N_e .

In the current work, we note that the model of Rajon and Masel (2011) contained an unrealistic symmetry, namely that the fitness consequence of a molecular error at one locus was exactly equal to that at any other loci. Here, we find that, with reasonable amounts of variation among loci (e.g., in their expression level or the per-molecule damage from their misfolded form), the bistability disappears. Intermediate solutions evolve instead, where cryptic deleterious sequences are purged only in more highly expressed genes, and quality control evolves to intermediate levels. Variation among loci does not change the previous finding that evolvability tracks the proportion of loci that contain a benign rather than a deleterious cryptic sequence.

The high rate of transcriptional error in *B. aphidicola* can be explained by adding a second bias toward deleterious mutations (in error rate), and hence a second drift barrier to our model. *B. aphidicola* and *E. coli* have high error rates for different reasons; high-fidelity quality control is redundant and unnecessarily expensive in *E. coli*, but unattainable in *B. aphidicola*, leading to similarly high transcriptional error rates.

Methods

Fitness

We follow the additive model of Rajon and Masel (2011), as outlined below, with a few important modifications to accommodate variation in gene expression levels. The model’s canonical example is the risk that a ribosome reads through a stop codon during translation.

The global mitigation strategy is to improve quality control of this gene expression subprocess. We assume that additional quality control that reduces the error rate, ρ , by some proportion, consumes a certain amount of time or comparable resource. Relative to a generation time of 1 in the absence of quality control costs, this gives generation time $1 + \delta \ln(1/\rho)$, where δ scales the amount of resources that could have been

used in reproduction, but are redistributed to quality control. Malthusian fitness is the inverse of generation time, giving

$$w_{QC} = \frac{1}{1 + \delta \ln(1/\rho)} \quad (1)$$

Following Rajon and Masel (2011), we set $\delta = 10^{-2.5}$, such that reducing ρ from 10^{-2} to 10^{-3} corresponds to a 0.7% reduction in fitness.

When a readthrough error happens, with frequency ρ , the consequences for fitness depend on the nature of the “cryptic sequence” that lies beyond the stop codon in the 3’UTR. The consequences of mistakes, mutational or otherwise, have a bimodal distribution, being either strongly deleterious (often lethal), or relatively benign, but rarely in between (Eyre-Walker and Keightley 2007; Fudala and Korona 2009). For example, a strongly deleterious variant of a protein might misfold in a dangerous manner, while a benign variant might fold correctly, although with reduced activity. We assume that alternative alleles of “cryptic genetic sequences” can be categorized according to a benign/deleterious dichotomy.

The local mitigation strategy, the alternative to global quality control, is thus for each cryptic sequence to evolve away from “deleterious” options and toward “benign” options. The local strategy of benign cryptic sequences has no direct fitness cost, but it is nevertheless difficult to evolve at so many loci at once. In contrast, expressing deleterious cryptic sequences has an appreciable cost. This cost scales both with the base rate of expression of the gene, and the proportion, ρ , of gene products that include the cryptic sequence.

Let the expression of gene i be E_i . We assign the concentration E_i of protein molecules of type i by sampling values of E_i from a \log_2 -normal distribution with standard deviation (SD) σ_E . We define D to be the total frequency of protein expression that would be highly deleterious if expressed in error:

$$D = \frac{\sum_{i \in \text{loci_with_del_crypt_seq}} E_i}{\sum_{i \in \text{loci}} E_i} \quad (2)$$

where the numerator sums only over loci that are deleterious, and the denominator sums over all loci. This normalization cancels out the effect of the mean value of E_i . We assume the costs of deleterious readthrough are additive across genes, based on the concept that misfolded proteins (Thomas *et al.* 1995) may aggregate in a nonspecific and harmful manner with other proteins and/or membranes (Kourie and Henry 2002), or may simply be expensive to dispose of (Goldberg 2003). After the stop codon is read through, translation will usually end at a backup stop codon within the 3’UTR. Under the assumption of additivity, readthrough events will reduce fitness by $c\rho D$, where c represents the strength of selection against misfolded proteins. Geiler-Samerotte *et al.* (2011) found that an increase in misfolded proteins of $\sim 0.1\%$ of total cellular protein molecules per cell imposed a cost of about 2% to relative growth rate. This gives an estimate of $c = 0.02/0.1\% = 20$.

Readthrough involving benign cryptic sequences does not incur this cost. However, when all cryptic sequences are benign (*i.e.*, $D = 0$), nothing stops ρ from increasing to unreasonably large values, *i.e.*, $\rho > 0.5$, which makes “erroneous” expression into the majority (and hence the “new normal”) form. This represents the antiredundancy solution of Krakauer and Plotkin (2002), in which any mutation has an extremely deleterious effect; indeed, as their per-locus penalty s (analogous to our ρcE) approaches 1, the fitness of their $k = 0$ genotype (analogous to our $D = 0$) approaches infinity. To avoid this scenario in our model of quality control, we add a cost in fitness $c\rho^2(1-D)$, whose impact is felt only at high values of ρ . One possible biological interpretation of this second order term is that, with probability ρ^2 , readthrough occurs not just through the regular stop codon, but also through the backup stop codon at the end of the benign cryptic genetic sequence. To reflect the effects of the double-error scenario under this interpretation, we therefore multiplied the second order term by the probability $\mu_{del}/(\mu_{del} + \mu_{ben})$ that a neutrally evolving cryptic sequence will be deleterious, where μ_{del} is the rate of deleterious-to-benign mutations, and μ_{ben} the reverse rate. Other double-error interpretations might involve different constants. In our case, the fitness component representing the cost of misfolded proteins is given by

$$w_{misfolding} = \max\left(0, 1 - c\rho D - c\rho^2(1 - D)\frac{\mu_{del}}{\mu_{del} + \mu_{ben}}\right) \quad (3)$$

Equation 3 is a natural extension of the additive model of Rajon and Masel (2011), generalizing to the case of variation in the degree of importance of cryptic loci. Where previous work referred to the number, L_{del} , of loci having the deleterious rather than benign form, we now distinguish between two measures, L_{del} and D , the latter reporting the proportion of gene product molecules rather than the number of gene loci.

Rajon and Masel (2011) also obtained near-identical results using a very different, multiplicative model. While this suggests that the exact function form of Equation 3 is unimportant, we chose the additive Equation 3 model as the more reasonable of the two options. The multiplicative model is premised on loss-of-function of the wild-type proteins, which likely has negligible impact for small losses of a protein whose activity is already close to saturation. In contrast, the additive model is premised on gain-of-negative-function effects of misfolded proteins. These plausibly constitute a major burden on fitness, through a combination of toxicity, disposal costs, and resources spent to replace a faulty molecule with a normal one.

To study evolvability, let a subset of K (typically 50) out of the L (typically ≥ 600) loci affect a quantitative trait, x , selection on which creates a third fitness component. Error-free expression of locus, k , occurring with frequency $1 - \rho$, has quantitative effect α_k , while expression that involves a benign version of the cryptic sequence has quantitative effect $\alpha_k + \beta_k$. Expression that involves a deleterious version of

the cryptic sequence is assumed to result in a misfolded protein that has no effect on the quantitative trait. We assume that expression level, E_k , is constant and already factored into values of α_k and β_k . This gives

$$x = \sum_k^K [(1 - \rho)\alpha_k + \rho B_k(\alpha_k + \beta_k)] \quad (4)$$

where $B_k = 1$ indicates a benign cryptic sequence, and $B_k = 0$ a deleterious one. As in Rajon and Masel (2011), we impose Gaussian selection on x relative to an optimal value x_{opt}

$$w_{trait}(x) = e^{-\frac{(x-x_{opt})^2}{2\sigma_f^2}} \quad (5)$$

where $\sigma_f = 0.5$.

Putting the three fitness components together, the relative fitness of a genotype is given by the product

$$w = w_{QC} \times w_{misfolding} \times w_{trait}. \quad (6)$$

Variance in expression levels

We estimated the variance in expression σ_E^2 from PaxDB (Wang *et al.* 2012, 2015), which is based on data released by the Global Proteome Machines (GMP) and other sources. We inferred σ_E equal to 2.24 (based on GMP 2012 release) or 3.31 (GMP 2014 release), for *S. cerevisiae*, and 2.93 (GMP 2014 release) for *Schizosaccharomyces pombe*. Note that, while our quantitative estimate of σ_E comes from variation in the expression levels of different proteins, consideration of variation along other lines might make a SD of 2.25 into a conservative underestimate of the extent of variation. See Supplemental Material, Figure B in File S1 for an exploration of this parameter value.

Mutation

There are six kinds of mutation: (1) conversion of a deleterious cryptic sequence to a benign form, (2) conversion from benign to deleterious, (3) change to the error rate, ρ , (4) change in the α value of one of the K quantitative trait genes, (5) change in the β value of one of those K genes, and (6) the co-option of a cryptic sequence to become constitutive, replacing the value of replacing α_k with that of $\alpha_k + \beta_k$ and reinitializing B_k and β_k .

It is this sixth kind of mutation that is responsible for the evolvability advantage of the local solution of benign cryptic sequences, providing more mutational raw material by which x might approach x_{opt} (Rajon and Masel 2011, 2013). The mutational co-option of a deleterious sequence ($B = 0$) is too strongly deleterious to be favored, even when replacing α_k and β_k might be advantageous. In other words, only benign cryptic sequences are available for mutational co-option. We use the term co-option of a 3'UTR readthrough sequence to refer to the case when a stop codon is lost by mutation, and not just read through by the ribosome (Giacomelli *et al.* 2007; Vakhrusheva *et al.* 2011; Andreatta *et al.* 2015). Mutational co-option for mimicking the consequences of errors other

than stop codon readthrough might involve mutations that change expression timing to make a rare protein–protein interaction common, or switch a protein’s affinity preference between two alternative partners.

Because we use an origin-fixation approach to simulate evolution (see below), only relative and not absolute mutation rates matter for our outcomes, with the absolute rates setting only the timescale—our rates are therefore effectively unitless. We use the same mutation rates as Rajon and Masel (2011), reduced 10-fold for convenience. Each locus with a benign cryptic sequence mutates to deleterious at rate $\mu_{del} = 2.4 \times 10^{-8}$, while deleterious loci mutate to benign less often, at rate $\mu_{ben} = 6 \times 10^{-9}$. Changes to the error rate ρ occur at rate, $\mu_{\rho} = 10^{-6}$, while the α and β values of quantitative loci each change with rates $\mu_{\alpha} = 3 \times 10^{-7}$ and $\mu_{\beta} = 3 \times 10^{-8}$, respectively. Mutational co-option occurs at each quantitative locus at rate $\mu_{coopt} = 2.56 \times 10^{-9}$.

Each mutation to ρ increases $\log_{10}\rho$ by an amount sampled from $\text{Normal}(\rho_{bias}, \sigma_{\rho}^2)$. By default, we set $\rho_{bias} = 0$ and $\sigma_{\rho} = 0.2$. To study extremely small populations with drift barriers to evolving even a global solution, we set $\rho_{bias} = 0.256$ and 0.465 , corresponding to ratios of ρ -increasing mutations: ρ -decreasing mutations of 9:1 and 99:1, respectively.

A similar scheme for α and β might create, in the global solution case of relaxed selection, a probability distribution of β whose variance increases in an unbounded manner over time (Lande 1975; Lynch and Gabriel 1983). Following previous work (Rajon and Masel 2011, 2013), we therefore let mutations alter α and β by an increment drawn from a normal distribution with mean $-\alpha/a$ or $-\beta/a$, with a set to 750, and with SD of σ_m/K in both cases, with σ_m set to 0.5. In the case of neutrality, this mutational process eventually reaches a stationary distribution with mean 0 and SD as calculated in Equation S3 of Rajon and Masel (2011):

$$V(a, K, \sigma_m) = \frac{(\sigma_m/K)^2}{1 - ((a-1)/a)^2} \quad (7)$$

A co-option at gene k changes the gene’s quantitative effect to

$$(1 - \rho)(\alpha_k + \beta_k) + \rho B'_k (\alpha_k + \beta_k + \beta'_k) \quad (8)$$

where B'_k and β'_k are the state and the quantitative effect of a new cryptic sequence created by co-option. Following a co-option mutation at locus k , we set the new B_k equal to 1 or 0, with probabilities proportional to μ_{ben} and μ_{del} , and resample the value of β_k from $\text{Normal}[0, V(a, K, \sigma_m)]$.

Evolutionary simulations by origin-fixation

We model evolution using an approach known as “weak mutation” (Gillespie 1983), or “origin-fixation” (McCandlish and Stoltzfus 2014). This approximation of population genetics is accurate in the limit where the waiting time until the appearance of the next mutation destined to fix is substantially longer than its subsequent fixation time. The population can then be approximated as genetically homogeneous in any

moment in time. While unrealistic for higher mutation rates and larger population sizes, origin-fixation models are computationally convenient. Still more importantly, origin-fixation models, unlike more realistic models with segregating variation, allow the location of the drift barrier to be set externally in the form of the value of the parameter, N , rather than having the location of the drift barrier emerge from complicated linkage phenomena within the model. Fortunately, for quantitative traits affected by multiple cryptic loci, most evolvability arises from diversity of the effects of co-option of different loci, rather than among the diversity of the effects of co-option from different starting genotypes (Rajon and Masel 2013). This allows us to study evolvability [in the population sense of Wagner (2008)], even in the absence of genetic diversity that is imposed by the origin-fixation formulation.

Our computationally efficient implementation of origin-fixation dynamics is described in detail in File S1, simulating a series of mutations that successively fix, and the waiting times between each.

Initialization and convergence

We initialized the trait optimum at $x_{opt} = 0$. We could have initialized all values of α_k and β_k at zero. However, at steady state, variance in $\sum_1^K \alpha_k$ and $\sum_1^K \beta_k$ is far lower than would be expected from variance in α_k and β_k —this emerges through a process of compensatory evolution (Rajon and Masel 2013). Allowing a realistic steady state to emerge in this way is computationally slow under origin-fixation dynamics, especially when N is large. We instead sampled the initial values of α_k and β_k from $\text{Normal}[0, V(a, K, \sigma_m)]$, where $V(a, K, \sigma_m)$ is defined by Equation 7, and then subtracted $\bar{\alpha}$ from α_k , and $\bar{\beta}$ from β_k , where $\bar{\alpha}$ and $\bar{\beta}$ are the means of a genotype across each of its quantitative loci, k . This process initializes α_k and β_k to have variances equal to those of the stationary distributions, while the overall trait value is initialized at the optimal value, zero. This procedure greatly reduces the burn-in computation time needed to achieve a somewhat subtle state of negative within-genotype among-loci correlations. We confirmed that subsequent convergence of the variance of $\sum_1^K \alpha_k$ was fast, occurring in <1000 steps, where a “step” is defined to be the fixation of one mutation. We expect $\log_{10}\rho$, D , and variance in β_k , to converge even faster than variance in α_k .

For the low- ρ initial conditions, ρ was initialized at 10^{-5} , and we initialized the benign vs. deleterious status of cryptic sequences at the neutral mutational equilibrium, choosing exactly $L \times \mu_{del}/(\mu_{del} + \mu_{ben})$ (rounded to the nearest integer) to be deleterious, independently of their different values of E . For the high- ρ initial conditions, we set ρ to 10^{-1} , and made all cryptic sequences benign.

We ran simulations for 10^5 steps, recording information at fixed times (measured in terms of waiting times), corresponding to approximately every 1000 steps on average, and hence yielding about 100 timepoints. To summarize the evolutionary outcome, we calculated the arithmetic means of $\log_{10}\rho$, of L_{del} , and of D among the last 20 timepoints, *i.e.*, approximating steps $0.8 \times 10^5 - 1 \times 10^5$.

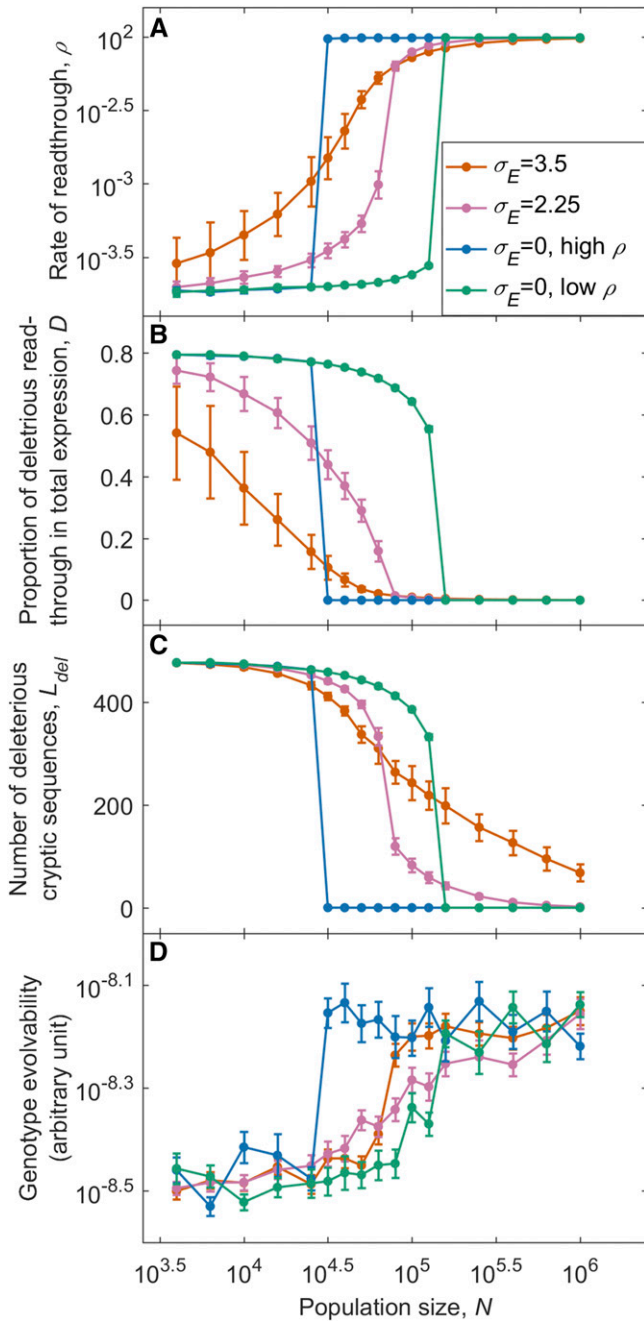


Figure 1 Evolutionary dynamics are bistable in the absence of variation in gene expression ($\sigma_E = 0$), but not with variation in gene expression ($\sigma_E = 2.25\text{--}3.5$). We calculated the average values of ρ , D , and L_{del} toward the end of the simulations, and then measured the genotype evolvability after changing the optimal trait value (see *Methods* for details). For each value of N , 20 simulations were initialized at high- ρ conditions, and 15 at low- ρ conditions. For $\sigma_E = 2.25\text{--}3.5$, simulations from the two initial conditions reached indistinguishable endpoints (Figure A in File S1), so the results were pooled. The increment in N is $10^{0.1}$ between $10^{4.4}$ and $10^{5.2}$ to increase resolution, and is $10^{0.2}$ elsewhere. At $\sigma_E = 0$, D is indistinguishable from zero for $N \geq 10^{5.2}$ under high- ρ conditions, and for $N \geq 10^{4.7}$ under low- ρ conditions, corresponding to L_{del} being effectively zero. In contrast, when $\sigma_E = 2.25$ or 3.5 , because the weakness of selection on low-expression genes prevents L_{del} from falling all the way to zero, D never quite reaches zero either, despite appearing superimposable in B. For (A–C), data are shown as mean \pm SD. For evolvability (D), data are

Evolvability

After adaptation to a trait optimum of $x_{opt} = 0$ had run to convergence (*i.e.*, after 10^5 steps), we changed x_{opt} to 2, forcing the quantitative trait to evolve rapidly. This allows the co-option of benign cryptic sequences an opportunity to increase evolvability. We measured evolvability in two ways: as the inverse of the waiting time before trait x exceeded 1, and the inverse of the waiting time before the population recovered half of the fitness it lost after x_{opt} changed. By default, we present results showing evolvability as time to fitness recovery; evolvability as time to trait recovery is shown only in Figure C in File S1.

We want our measures of evolvability to reflect a genotype’s potential to generate beneficial mutations, but this goal was complicated by population size. A large population finds a given beneficial mutation faster than does a small population, inflating the total fixation flux $\sum_{i \in \text{beneficial_mutation}} \mu_i N P_{fix}(i)$, where μ_i is the influx of mutations of beneficial type i and P_{fix} is their probability of fixation (the latter described by Equation 9 in File S1), in direct proportion to population size. We therefore divided our evolvability measures by the population size to correct for this effect. This normalization converts the population-level evolvability measure into a measure of the population-size-independent evolvability of a single individual that has the genotype of interest.

Data availability

Source code for the simulations is available at <https://github.com/MaselLab/>. All simulations were run with Matlab (R2014a).

Results

Recall that, in the absence of variation in expression among genes, there are two solutions to handle erroneous expression due to stop codon readthrough: at high population size N , the local solution purges all deleterious cryptic sequences, making high rates of readthrough harmless, while, at low N , the global solution reduces the rate of readthrough, allowing deleterious cryptic sequences to accumulate near-neutrally. At intermediate N , we see bistability, with either solution possible, depending on starting conditions (Figure 1, $\sigma_E = 0$). It is important to note that we use the word “bistability” loosely. Strictly speaking, bistability means that the system has two stable steady states (here a state is defined by readthrough rate and the exact property of each cryptic sequence), *i.e.*, two attractors. But, in a stochastic model, there are no attractors in the strict sense of the word, only a stationary distribution of states. We use the term bistability to refer to the case where the stationary distributions of states have two modes. Transitions between the two modes are rare, therefore the two modes can be loosely interpreted as the two attractors of the system.

shown as mean \pm SE. For (A) and (D), these apply to log-transformed values. Evolvability is based on time to fitness recovery; see Figure C in File S1 for similar results based on time to trait recovery. $L = 600$.

Our results qualitatively reproduce the bistability reported by Rajon and Masel (2011) for the case where there is no expression variation among genes, though the range of values of N leading to bistability is smaller than that found in Rajon and Masel (2011), in which a full Wright-Fisher simulation is used. The smaller range of bistability in our model could be caused by the ease with which long-term evolution is captured using an origin-fixation framework, or by other subtle differences between the approaches, *e.g.*, the greater ease of compensatory evolution under Wright-Fisher dynamics than under origin-fixation. We chose origin-fixation mainly to reduce the computational burden, which for our study was increased by the need to track individual loci, in contrast to previous work that needed only to track the number of loci with deleterious cryptic sequence, without distinguishing their identities (Rajon and Masel 2011, 2013).

However, bistability vanishes with variation in expression among genes (Figure 1, $\sigma_E = 2.25$ and $\sigma_E = 3.5$). To understand why, consider a population initialized at low readthrough rate (ρ) and many deleterious cryptic sequences. Because the strength of selection against a deleterious cryptic sequence at locus i is proportional to ρE_i (the effect of a locus i on D in Equation 3 is proportional to E_i), purging works at the most highly expressed loci, even when ρ is low. This lowers the proportion D of readthrough events that are deleterious, which relaxes selection for high fidelity, leading to an increase in ρ . As ρ increases, loci with lower E_i become subject to effective purging, which further reduces D , which feeds back to increase ρ further. Because E_i is log-normally distributed, but contributes linearly to selection via D , each round of the feedback loop involves smaller changes than the last. Eventually, the changes are too small for selection on them to overcome mutation bias in favor of deleterious sequences. Similarly, when a population is initialized at high ρ , mutational degradation begins at low E_i sites, and arrests when selection is strong enough to kick in. The point of balance between mutation bias and selection defines a single intermediate attractor for $\sigma_E \geq 2.25$, instead of the bistable pair of attractors found for uniform E_i ($\sigma_E = 0$). For $\sigma_E < 2.25$, bistability is still found, but for a narrower range of population sizes than in the absence of variation (Figure B in File S1).

Even though bistability is not found for $\sigma_E = 2.25$, there is still a fairly sharp dichotomy, with solutions being either local (high ρ and low L_{del}) or global (low ρ and high L_{del}), and intermediate solutions found only for a very restrictive range of N , following a sigmoidal curve (Figure 1, A and C). Increasing variation in expression among genes blurs the boundary between the local solution and the global solution. Intermediate solutions are found for broader ranges of N as expression variance σ_E increases to 3.5. The trend, as expression variance σ_E increases from 0, is to first replace bistability with a limited range of intermediate solutions ($\sigma_E = 2.25$), and then for the intermediate solutions to become more prevalent, with extreme local and global solutions becoming less attainable as $\sigma_E > 2.25$.

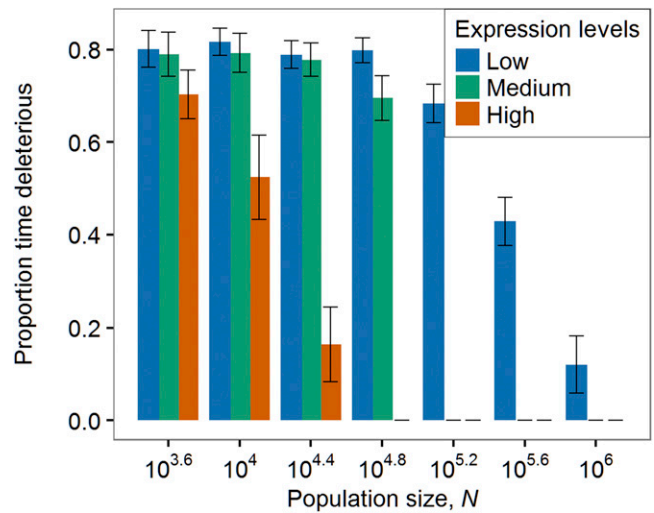


Figure 2 The effectiveness of purging a cryptic sequence of deleterious mutations depends on its expression level. We examined the states of the cryptic sequences of the loci with the 10 highest, the 10 lowest, and the 10 median expression levels among the 600 loci in each of the simulations shown in Figure 1 ($\sigma_E = 2.25$). We counted how often each locus contained a deleterious cryptic sequence among the last 20 timepoints we had collected from that simulation. Bars represent the proportion of time that each of the 10 loci carried a deleterious cryptic sequence, averaged over 20 replicates, and shown as mean \pm SD. Simulations were initialized at low- ρ conditions.

The breakdown of the local solution begins with intermediate values of L_{del} , while the breakdown of the global solution begins with intermediate values of ρ and D (Figure 1, A–C). The breakdown of global solutions involves high-expression loci (Figure 2), which affect D more than L_{del} . In contrast, the breakdown of local solutions involves low-expression loci (Figure 2), which affect L_{del} more than D . Because ρ is better described as coevolving with D than with L_{del} , as explained earlier, intermediate values of ρ are seen more in the breakdown of global than local solutions.

A primary motivation behind characterizing the two solutions is that the local solution was found to have dramatically higher evolvability than the global solution (Rajon and Masel 2011). We therefore check whether this conclusion still broadly stands in the presence of variation in expression levels. The local solution promotes evolvability by making benign cryptic sequences available for co-option. Differences in evolvability between genotypes should therefore be largely determined by the fraction of quantitative trait loci that carry benign, rather than deleterious, cryptic sequences. In agreement with this, evolvability inversely mirrors L_{del} , as a function of population size, *i.e.*, evolvability (Figure 1D) resembles L_{del} (Figure 1C) far more than it resembles ρ (Figure 1A) or D (Figure 1B).

The distinction between global and local solutions becomes more extreme when the mutation bias toward deleterious rather than benign cryptic sequences is increased from a 4:1 ratio to a 99:1 ratio, but persists even when the mutation bias is eliminated in favor of a 1:1 ratio (Figure 3). In the absence of

mutation bias, there is less evolvability to be gained by the local relative to the global solution, since half the quantitative loci are available for co-option regardless (Figure 3C). Nevertheless, a small evolvability advantage to the local solution can still be observed (Figure 3D). In any case, assuming mutation bias toward deleterious options is biologically reasonable, and Figure 3 shows that results are not sensitive to the quantitative strength of our assumption on this count.

When we also account for mutation bias that tends to increase rather than decrease the error rate ρ , our model can explain the previously puzzling observation that the rate of transcriptional errors in small- N_e endosymbiont bacteria *Buchnera* is so much higher than that of *C. elegans*, and almost as high as that of large- N_e *E. coli* (McCandlish and Plotkin 2016; Traverse and Ochman 2016b). In extremely small populations, even the global solution is subject to a drift barrier, making ρ higher than its optimal value. For N so small such that most ρ -increasing mutations pass through the drift barrier, ρ can be almost as large as that in large populations (Figure 4A). Despite their high error rates, these extremely small populations also carry heavy drift loads of deleterious cryptic products (Figure 4, B and C), consistent with the fact that in *B. aphidicola*, unlike *E. coli*, selection is unable to reduce the fraction of nonsynonymous transcriptional errors that are nonsynonymous (Traverse and Ochman 2016a). High ρ shows the absence of a global solution, while high D and L_{del} show the absence of a local solution; neither solution is found for a sufficiently small population. Similar error rates in large and small populations can also be found, given bias in mutations to ρ , when there is no variation in expression levels (Figure E in File S1).

The parameters in our model can be classified into three groups, and the exploration of their values is summarized in Table A in File S1. The first group controls selection coefficients relevant to the global vs. local solution outcome: the variance in expression levels (σ_E^2), the number of loci (L , Figure D in File S1), the cost of misfolded protein molecules (c), and the cost of quality control (δ , Figure F in File S1). The second group controls mutation bias relevant to the global vs. local solution outcome: the frequency with which mutations turn deleterious cryptic sequences benign vs. the reverse ($\mu_{ben}:\mu_{del}$), whether mutations to ρ tend to increase or decrease it ($P_{+\rho}:P_{-\rho}$), and variance in the magnitude of mutations to ρ (σ_ρ^2 , Figure G in File S1). The third group contains all the parameters that control the evolution of quantitative traits encoded by a minority of loci relevant to the evolvability properties. Because our focus in this manuscript is on the evolution of global vs. local solutions, not on the precise details of the relationship between local solutions and evolvability, these parameter values were explored less.

The influence of σ_E^2 dominates our results. Its effect in eliminating bistability holds, with the one exception that very “cheap” quality control could partially restore bistability (Figure F in File S1). Otherwise, we found that three parameters— c , δ , and $\mu_{ben}:\mu_{del}$ —are the main determinants of the population size at which the transition between global

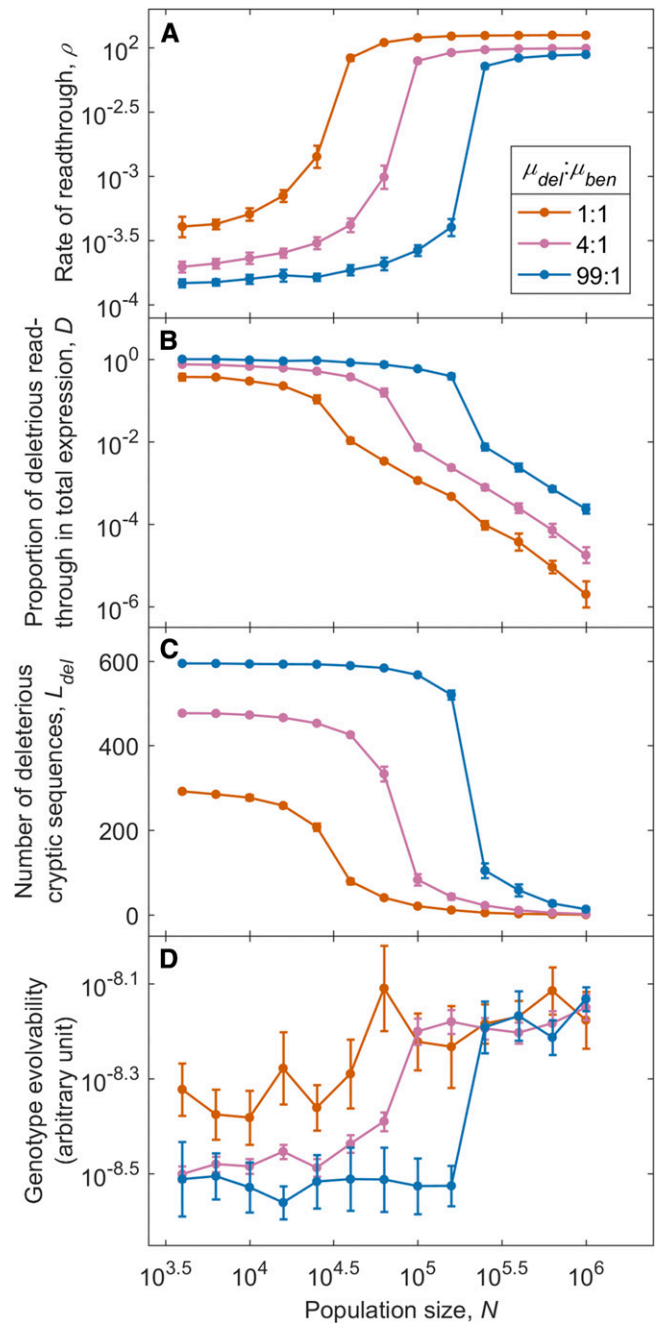


Figure 3 Results become more extreme when the mutation bias in the state of a cryptic sequence is increased from a 4:1 ratio to a 99:1 ratio, but do not disappear completely when the mutation bias is eliminated in favor of a 1:1 ratio. The location of the drift barrier shifts as a function of mutation bias, but the dichotomy between local and global solutions (as seen in values of ρ and D) is not sensitive to relaxing the mutation bias. The advantage of the local solution with respect to evolvability [as seen in (D) and mirrored in L_{del} (C)] is more sensitive to lack of mutation bias, but is still visible even with a 1:1 ratio. To compare results across different mutation biases, we kept the sum of the two mutation rates constant. For the low- ρ initial conditions, the number of deleterious cryptic sequences was initialized at the neutral mutational equilibrium of $L \times \mu_{del}/(\mu_{del} + \mu_{ben})$ (rounded to the nearest integer). For $\mu_{del}:\mu_{ben} = 4:1$, we reused the results shown in Figure 1. For the other ratios, five replicates were run for each initial condition, and pooled. For (A–C), data are shown as mean \pm SD. For (D), data are shown as mean \pm SE. For (A) and (D), these apply to log-transformed values. $L = 600$ and $\sigma_E = 2.25$.

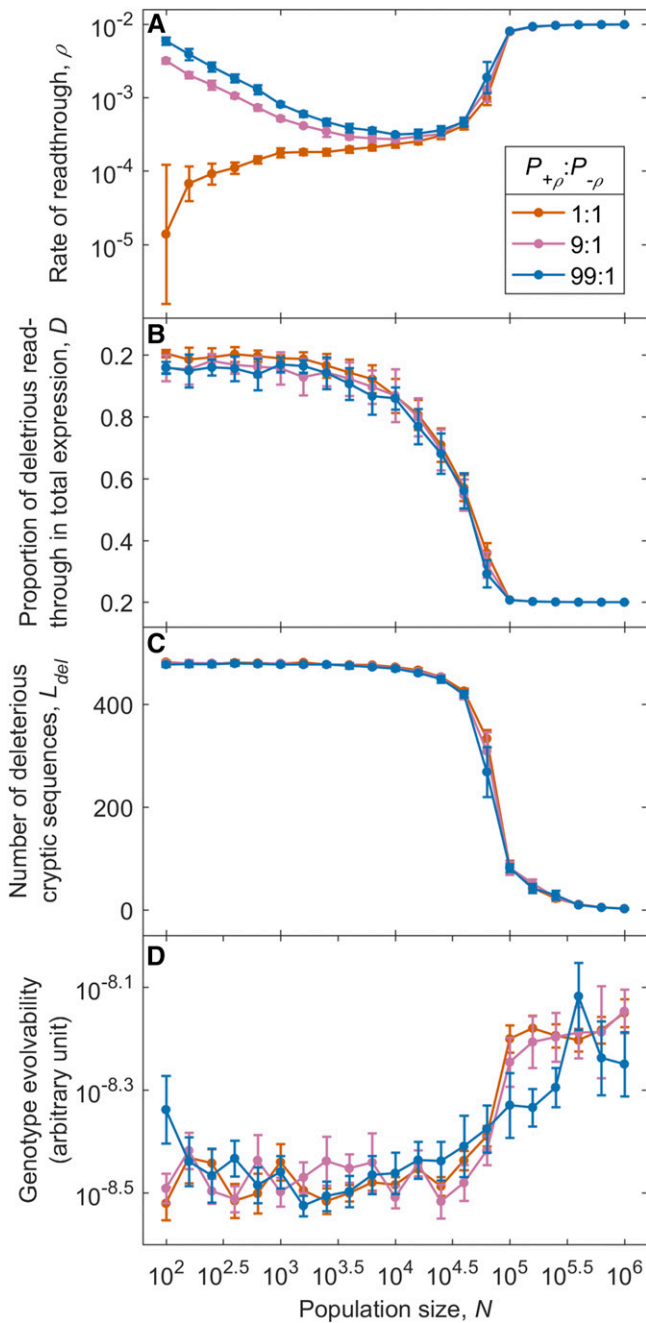


Figure 4 Mutation bias tends to increase ρ , such that even the global solution breaks down in sufficiently small populations. $P_{+\rho}$ is the probability that a mutation increases ρ , and $P_{-\rho}$ is the probability of a decrease. Each data point, (except those taken from Figure 1 with $P_{+\rho}:P_{-\rho} = 1:1$ and $N = 10^{3.6}-10^{6.0}$), is pooled from five replicates of high- ρ initial conditions and five replicates of low- ρ initial conditions. Because we assume multiplicative mutational effects to ρ , its value converges even for extremely small N . *i.e.*, as ρ increases, the additive effect size $\Delta\rho$ of a typical mutation also increases, preventing it from passing through the drift barrier. For (A–C), data are shown as mean \pm SD. For (D), data are shown as mean \pm SE. For (A) and (D), these apply to log-transformed values. $L = 600$ and $\sigma_E = 2.25$.

and local solutions takes place, and of the exact error rate that evolves for global and local solutions (Table A in File S1). The other parameters in the first and second groups have

little or no influence on the evolutionary outcomes that we study. In general, parameters in the first group, controlling selection, have stronger effects than the second group, controlling mutation bias.

Discussion

When genes vary in their expression levels, the dichotomy between the local and global solutions is replaced by a continuous transition. Very large populations still resemble the local solution, although mutations making cryptic sequences deleterious still pass through the drift barrier in the occasional low-expression gene. Very small populations still resemble the global solution, although mutations making cryptic sequences deleterious may still be effectively purged in a few high-expression genes; because their high expression disproportionately affects the burden from misexpression, this relaxes expression for high fidelity, leading to less strict quality control.

In agreement with drift barrier theory, large- N_e *E. coli* exhibits a local solution—a tendency for transcription errors to have synonymous effects—while small- N_e *B. aphidicola* does not (Traverse and Ochman 2016a). While, as predicted, the global solution of low transcriptional error rates does not obey the naïve drift barrier expectation of being higher in *B. aphidicola* than in *E. coli* (Traverse and Ochman 2016a), nor are transcription error rates drastically lower in *B. aphidicola* as predicted by previous theory on the interplay between global and local solutions (Rajon and Masel 2011; McCandlish and Plotkin 2016). This significantly lower rate relative to *E. coli* is, however, found in intermediate- N_e *C. elegans*. Where previous work (Rajon and Masel 2011) explained only the relative rates for *E. coli* and *C. elegans*, here we also explain the high error rate of *B. aphidicola* by taking into account a drift barrier on the global solution of low error rates. This drift barrier is significant because of mutation bias toward higher error rates. Small *B. aphidicola* populations have higher error rates than *C. elegans* because it is the best that evolution at low N_e can manage, despite the deleterious consequences; large *E. coli* populations have similarly high error rates because, with the worst consequences of error already purged, they do not need to incur the cost that quality control entails.

With small amounts of variation in expression among genes, the range of intermediate values of N_e for which bistability is found shrinks. With more variation, bistability vanishes in favor of a sigmoidal transition between global and local solutions. With still more, the sigmoid is smoothed out, and intermediate solutions are found for most values of N_e .

To interpret our results correctly, we must therefore estimate the degree to which genes vary. The results presented here focus on two estimates of the variance in log-expression in yeast, namely σ_E of 2.25 and 3.5. However, variation among genes in the deleterious consequences of misfolding, in addition to variation in expression levels, might make larger σ_E a better model of reality, further supporting a continuum of

intermediate solutions. In other words, the value of c in Equation 3 may vary among genes. Note that apart from the second-order ρ^2 term, the cost of a deleterious misfolded protein i depends only on the product of c_i and expression level E_i . Given log-normal distributions of c_i and expression level E_i , the variance of the log-product is equal to the sum of the two log-variances, so we can transform this scenario into one where c is constant, and σ_E^2 is equal to this sum. This can be done because changing c_i and E_i only affects $w_{\text{misfolding}}$, and not other factors such as the magnitude of a locus's influence on the quantitative trait. In other words, adding variation to c is almost equivalent to increasing the variance in expression levels.

The values of μ_{del} and μ_{ben} may also vary among genes. Drift barrier effects operate via the effect of population size on the fate of deleterious not beneficial mutations—if purging is efficient, then the beneficial mutation rate does not matter, because a single beneficial mutation is enough. We therefore focus on μ_{del} . The inclusion of a benign-to-deleterious mutation M_i at locus i depends on the product of μ_{del} at locus i and M_i 's probability of fixation. It seems likely that variation among genes in the probability that a deleterious cryptic sequence becomes fixed will swamp variation in the deleterious mutation rate—variation in expression levels causes the former to vary over orders of magnitude. Note that, as for the case of variation in c , it is possible to construct a manipulation of E_i that has the same effect on the relevant product, via the probability of fixation, as would occur given a change in μ_{del} . While this case is less neat than for the product $c_i E_i$, it illustrates that a model of variation in expression levels can reflect, to some extent, the effect of variation in μ_{del} .

Our model makes three critical assumptions, which must be understood for the results to be interpreted appropriately. First, a “locus” in our model consists of one regular and one cryptic sequence. The primary example that we used to parameterize the simulations posits an entire protein-coding gene as the regular sequence, and the extended polypeptide resulting from stop codon readthrough as the cryptic alternative. In the example of transcriptional errors, a locus is a single codon, with its corresponding amino acid being the regular sequence, and the most common consequence of a transcriptional error as the cryptic. The case of one regular sequence and many alternative cryptic ones has not been modeled. Similarly, proteins may each have a regular fold or binding partner, and our model considers the contrast between this state and a single cryptic alternative.

Second, we assume that the rate of gene expression errors is set globally, across all loci. In reality, individual context may also affect the error rate, giving error rates a local solution aspect as well. A model of three rather than two interacting solutions—global error rates, local error rates, and local robustness to the consequences of error—remains for future work. Perhaps highly expressed genes will have both more benign cryptic sequences and lower rates of error, or perhaps the evolution of one kind of local solution will alleviate the need for another. Testing this empirically requires data on

site-specific error rates, and on a credible marker for the benign status of members of an identifiable class of cryptic sequences. Such tools are now becoming available, and indeed we recently found a positive correlation between a large number of readthrough errors at a particular stop codon and the benign status of the readthrough translation product (L. J. Kosinski *et al.* unpublished results). We also reanalyzed the data of Traverse and Ochman (2016a) to find that highly expressed transcripts have lower transcriptional error rates (K. Meer *et al.* unpublished results).

Finally, we assume that the consequences of errors have a bimodal distribution: either highly deleterious or largely benign, but rarely in between. In other words, we assume that a basic phenomenon in biology is that changes tend to either break something, or to tinker with it. There are a variety of lines of evidence supporting this intuitively reasonable assumption (Fudala and Korona 2009; Wylie and Shakhnovich 2011).

Acknowledgments

We thank Lilach Hadany, Yoav Ram, and other members of the Hadany group for helpful discussions that prompted us to explore variation in expression. We thank Paul Nelson for developing the idea of local error rates as an expansion of our model, Ben Wilson for help with R, and Etienne Rajon, Yoav Ram, Tobias Warnecke, and one anonymous reviewer, for helpful comments on the manuscript. We also thank Charles Traverse and Howard Ochman for sharing their data on transcriptional errors. An allocation of computer time from the University of Arizona Research Computing High Performance Computing (HPC) and High Throughput Computing (HTC) at the University of Arizona is gratefully acknowledged. This work was supported by the John Templeton Foundation [grant number 39667]. D.J.P. was also funded by the Undergraduate Biology Research Program at the University of Arizona.

Literature Cited

- Adachi, M., and A. R. O. Cavalcanti, 2009 Tandem stop codons in ciliates that reassign stop codons. *J. Mol. Evol.* 68: 424–431.
- Andreatta, M. E., J. A. Levine, S. G. Foy, L. D. Guzman, L. J. Kosinski *et al.*, 2015 The recent de novo origin of protein C-termini. *Genome Biol. Evol.* 7: 1686–1701.
- Brettner, L. M., and J. Masel, 2012 Protein stickiness, rather than number of functional protein-protein interactions, predicts expression noise and plasticity in yeast. *BMC Syst. Biol.* 6: 128.
- Drummond, D. A., and C. O. Wilke, 2008 Mistranslation-induced protein misfolding as a dominant constraint on coding-sequence evolution. *Cell* 134: 341–352.
- Eyre-Walker, A., and P. D. Keightley, 2007 The distribution of fitness effects of new mutations. *Nat. Rev. Genet.* 8: 610–618.
- Frank, S. A., 2007 Maladaptation and the paradox of robustness in evolution. *PLoS One* 2: e1021.
- Fudala, A., and R. Korona, 2009 Low frequency of mutations with strongly deleterious but nonlethal fitness effects. *Evolution* 63: 2164–2171.

- Geiler-Samerotte, K. A., M. F. Dion, B. A. Budnik, S. M. Wang, D. L. Hartl *et al.*, 2011 Misfolded proteins impose a dosage-dependent fitness cost and trigger a cytosolic unfolded protein response in yeast. *Proc. Natl. Acad. Sci. USA* 108: 680–685.
- Giacomelli, M. G., A. S. Hancock, and J. Masel, 2007 The conversion of 3' UTRs into coding regions. *Mol. Biol. Evol.* 24: 457–464.
- Gillespie, J. H., 1983 Some properties of finite populations experiencing strong selection and weak mutation. *Am. Nat.* 121: 691–708.
- Goldberg, A. L., 2003 Protein degradation and protection against misfolded or damaged proteins. *Nature* 426: 895–899.
- Good, B. H., and M. M. Desai, 2014 Deleterious passengers in adapting populations. *Genetics* 198: 1183–1208.
- Gout, J.-F., W. K. Thomas, Z. Smith, K. Okamoto, and M. Lynch, 2013 Large-scale detection of in vivo transcription errors. *Proc. Natl. Acad. Sci. USA* 110: 18584–18589.
- Kimura, M., T. Maruyama, and J. F. Crow, 1963 The mutation load in small populations. *Genetics* 48: 1303–1312.
- Kourie, J. I., and C. L. Henry, 2002 Ion channel formation and membrane-linked pathologies of misfolded hydrophobic proteins: the role of dangerous unchaperoned molecules. *Clin. Exp. Pharmacol. Physiol.* 29: 741–753.
- Krakauer, D. C., and J. B. Plotkin, 2002 Redundancy, antiredundancy, and the robustness of genomes. *Proc. Natl. Acad. Sci. USA* 99: 1405–1409.
- Lande, R., 1975 The maintenance of genetic variability by mutation in a polygenic character with linked loci. *Genet. Res.* 26: 221–235.
- Liang, H., A. R. O. Cavalcanti, and L. F. Landweber, 2005 Conservation of tandem stop codons in yeasts. *Genome Biol.* 6: R31.
- Lynch, M., 2007 *The origins Of Genome Architecture*. Sinauer Associates, Sunderland, MA.
- Lynch, M., 2010 Evolution of the mutation rate. *Trends Genet.* 26: 345–352.
- Lynch, M., 2012 Evolutionary layering and the limits to cellular perfection. *Proc. Natl. Acad. Sci. USA* 109: 18851–18856.
- Lynch, M., and W. Gabriel, 1983 Phenotypic evolution and parthenogenesis. *Am. Nat.* 122: 745–764.
- McCandlish, D. M., and A. Stoltzfus, 2014 Modeling evolution using the probability of fixation: history and implications. *Q. Rev. Biol.* 89: 225–252.
- McCandlish, D. M., and J. B. Plotkin, 2016 Transcriptional errors and the drift barrier. *Proc. Natl. Acad. Sci. USA* 113: 3136–3138.
- Mira, A., and N. A. Moran, 2002 Estimating population size and transmission bottlenecks in maternally transmitted endosymbiotic bacteria. *Microb. Ecol.* 44: 137–143.
- Nichols, J. L., 1970 Nucleotide sequence from the polypeptide chain termination region of the coat protein cistron in bacteriophage R17 RNA. *Nature* 225: 147–151.
- Rajon, E., and J. Masel, 2011 The evolution of molecular error rates and the consequences for evolvability. *Proc. Natl. Acad. Sci. USA* 108: 1082–1087.
- Rajon, E., and J. Masel, 2013 Compensatory evolution and the origins of innovations. *Genetics* 193: 1209–1220.
- Rispe, C., F. Delmotte, R. C. H. J. van Ham, and A. Moya, 2004 Mutational and selective pressures on codon and amino acid usage in *Buchnera*, endosymbiotic bacteria of aphids. *Genome Res.* 14: 44–53.
- Thomas, P. J., B.-H. Qu, and P. L. Pedersen, 1995 Defective protein folding as a basis of human disease. *Trends Biochem. Sci.* 20: 456–459.
- Traverse, C. C., and H. Ochman, 2016a Conserved rates and patterns of transcription errors across bacterial growth states and lifestyles. *Proc. Natl. Acad. Sci. USA* 113: 3311–3316.
- Traverse, C. C., and H. Ochman, 2016b Correction for Traverse and Ochman, conserved rates and patterns of transcription errors across bacterial growth states and lifestyles. *Proc. Natl. Acad. Sci. USA* 113: E4257–E4258.
- Vakhrusheva, A., M. Kazanov, A. Mironov, and G. Bazykin, 2011 Evolution of prokaryotic genes by shift of stop codons. *J. Mol. Evol.* 72: 138–146.
- Wagner, A., 2008 Robustness and evolvability: a paradox resolved. *Proc. Biol. Sci.* 275: 91–100.
- Wang, M., M. Weiss, M. Simonovic, G. Haertinger, S. P. Schrimpf *et al.*, 2012 PaxDb, a database of protein abundance averages across all three domains of life. *Mol. Cell. Proteomics* 11: 492–500.
- Wang, M., C. J. Herrmann, M. Simonovic, D. Szklarczyk, and C. von Mering, 2015 Version 4.0 of PaxDb: protein abundance data, integrated across model organisms, tissues, and cell-lines. *Proteomics* 15: 3163–3168.
- Warnecke, T., and L. D. Hurst, 2011 Error prevention and mitigation as forces in the evolution of genes and genomes. *Nat. Rev. Genet.* 12: 875–881.
- Williams, I., J. Richardson, A. Starkey, and I. Stansfield, 2004 Genome-wide prediction of stop codon readthrough during translation in the yeast *Saccharomyces cerevisiae*. *Nucleic Acids Res.* 32: 6605–6616.
- Wu, X., and L. D. Hurst, 2015 Why selection might be stronger when populations are small: intron size and density predict within and between-species usage of exonic splice associated cis-Motifs. *Mol. Biol. Evol.* 32: 1847–1861.
- Wylie, C. S., and E. I. Shakhnovich, 2011 A biophysical protein folding model accounts for most mutational fitness effects in viruses. *Proc. Natl. Acad. Sci. USA* 108: 9916–9921.

Communicating editor: J. Hermisson

Supplemental material for the manuscript

“Drift barriers to quality control when genes are expressed at different levels”

Xiong K, McEntee JP, Porfirio DJ, Masei J

Implementation of origin-fixation simulations

Origin-fixation models are often implemented via a crude rejection algorithm; large numbers of mutations are simulated, and each is accepted as a successful fixation event if and only if a random number sample from the uniform [0, 1] distribution falls below its (fairly low) fixation probability. For large N , this method is computationally slow when significant numbers of nearly neutral mutations must be sampled before one fixes with probability $\sim 1/N$. Given that our model posits only a relatively small range of possible mutations, we instead sampled only mutations that go on to become fixed, by sampling according to the relative values of “fixation flux”, proportional to mutation rate \times fixation probability for each of our six categories of mutation. In other words, we used a form of the Gillespie (1977) algorithm.

In a haploid population of size N , the probability of fixation of a new mutant into a resident population is given by

$$P_{fix} = \frac{1-e^{-s}}{1-e^{-Ns}} \quad (9)$$

where $s = w_{mutant}/w_{resident}-1$. It is then straightforward to calculate fixation flux values for all possible switches between benign and deleterious states:

$$f_{del_to_ben} = N\mu_{ben} \sum_{i \in loci_with_del_crypt_seq} P_{fix}(del_to_ben_at_i) \quad (10)$$

$$f_{ben_to_del} = N\mu_{del} \sum_{i \in loci_with_ben_crypt_seq} P_{fix}(ben_to_del_at_i) \quad (11)$$

Matters are slightly more complicated for quantitative mutations to α , β and ρ , because we must integrate the fixation flux over all possible sizes ($\Delta\alpha_k$, $\Delta\beta_k$, and $\Delta\log_{10}\rho$) for a mutation at a given locus, prior to summing across loci to arrive at the fixation flux for an entire mutational category:

$$f_\alpha = N\mu_\alpha \sum_k^K \int P_{fix}(\Delta\alpha_k)P(\Delta\alpha_k)d\Delta\alpha_k \quad (12)$$

$$f_\beta = N\mu_\beta \sum_k^K \int P_{fix}(\Delta\beta_k)P(\Delta\beta_k)d\Delta\beta_k \quad (13)$$

$$f_\rho = N\mu_\rho \int P_{fix}(\Delta\log_{10}\rho)P(\Delta\log_{10}\rho)d\Delta\log_{10}\rho \quad (14)$$

where $P(\Delta\alpha_k)$, $P(\Delta\beta_k)$, and $P(\Delta\log_{10}\rho)$ are the probability densities for the magnitude of a given kind of mutation.

We use the quadrature method to calculate the integral over these possibilities, using a grid of 2000, limited for $\Delta\alpha_k$ to the interval $[-\alpha_k/a-5\sigma_m/K, -\alpha_k/a+5\sigma_m/K]$, for $\Delta\beta_k$ to the interval $[-\beta_k/a-5\sigma_m/K, -\beta_k/a+5\sigma_m/K]$, and for $\Delta\log_{10}\rho$, to the interval $[-10\sigma_\rho, \min(10\sigma_\rho, -\log_{10}\rho)]$. In the latter case, the number of grid intervals is reduced proportional to any truncation of the interval at $-\log_{10}\rho$.

For mutational co-options of benign cryptic sequences, the effect of replacing the value of α_k with that of $\alpha_k + \beta_k$ is fixed, but there is also a stochastic range of effects of initializing a new β_k and a new B_k (Eq. 15). Let $P(\beta'_k)$ be the probability density of a new β_k given by Normal(0, $V(a, K, \sigma_m)$), and $P(B'_k = 1) = 1 - P(B'_k = 0)$ be the probability that a new B_k equals to 1, and hence the new β_k affects the trait value. The fixation flux associated with cooption mutations we obtained numerically by integration over the range $[-5\sigma_m/K, 5\sigma_m/K]$:

$$f_{coopt} = N\mu_{coopt} \sum_{k \in \text{loci_with_ben_crypt_seq}}^K \left(P(B'_k = 1) \int P_{fix}(\beta'_k, B'_k = 1) P(\beta'_k) d\beta'_k + P(B'_k = 0) P_{fix}(B'_k = 0) \right) \quad (15)$$

The expected waiting time before the current genotype is replaced by another is

$$\text{waiting time} = \frac{1}{\text{total fixation flux over all six categories}} \quad (16)$$

A standard Gillespie (1977) algorithm would calculate the realized waiting time as a random number drawn from an exponential distribution with this mean. Since we are only interested in the outcome of evolution, and not the variation in its timecourse, we used the expected waiting time instead, decreasing our computation time. The waiting time can be interpreted as the time it takes for a mutation destined for fixation to appear, neglecting the time taken during the process of fixation itself. Using this interpretation, we specify waiting times in terms of numbers of generations, based on our assumptions about absolute mutation rates.

We assign the identity of the next fixation event among the six categories according to probabilities proportional to their relative fixation fluxes, then we assign the identity within the category. For switches between benign and deleterious states, allocating a fixation event within a category according to the relative values of fixation fluxes is straightforward. For mutations to ρ , α , and β , and mutational co-option, we relax the granularity and cutoff assumptions of the grid-integration method when choosing a mutation within the category. Instead, we sample a mutational value of $\Delta\log_{10}\rho$ from $\text{Normal}(\rho_{bias}, \sigma_{\rho}^2)$. We reject and resample $\Delta\log_{10}\rho$ if $\Delta\log_{10}\rho \geq -\log_{10}\rho$. Otherwise, we accept vs. reject-resample according to the fixation probability of that exact mutation, by comparing this probability to a random number uniformly distributed at $[0, 1.1 \times \text{the maximum fixation probability across the grid points previously calculated for } \Delta\log_{10}\rho \text{ during our grid calculation}]$. For $\Delta\alpha$ (or $\Delta\beta$), the procedure is conceptually similar but has a more complicated implementation. We first sample from $\text{Normal}(0, (\sigma_m / K)^2)$. We then add the random number to each of the values of $-\alpha_k/a$, and calculate the sum of corresponding fixation probabilities across all loci k . We accept vs. reject-resample the mutation by comparing this sum to a random sample from a uniform distribution at $[0, 1.1 \times \text{the maximum corresponding fixation probability sum calculated during our grid calculation}]$. If the mutation is accepted, we allocate it to a locus k with probability proportional to their relative fixation probabilities. For mutational co-option of a benign cryptic sequence, the main effect is to replace α_k with $\alpha_k + \beta_k$, but there are also subtler effects arising from the reinitialization of the new cryptic sequence. Any of the k loci for which $B = 1$ are eligible for co-option, the new value of B may be either 0 to 1, and the new β_k may take a range of values. Each combination of k and new B has its own fitness flux, and the first choice is among these $\{k, B\}$ pairs. Next we sample

β_k from Normal(0, $(\sigma_m/k)^2$); for a new B equal to 0 we always accept the result, and for new B equal to 1, we accept vs. reject-resample β_k by comparing its probability of fixation to a random sample from a uniform distribution at $[0, 1.1 \times \text{the maximum corresponding fixation probability sum calculated during our grid calculation}]$.

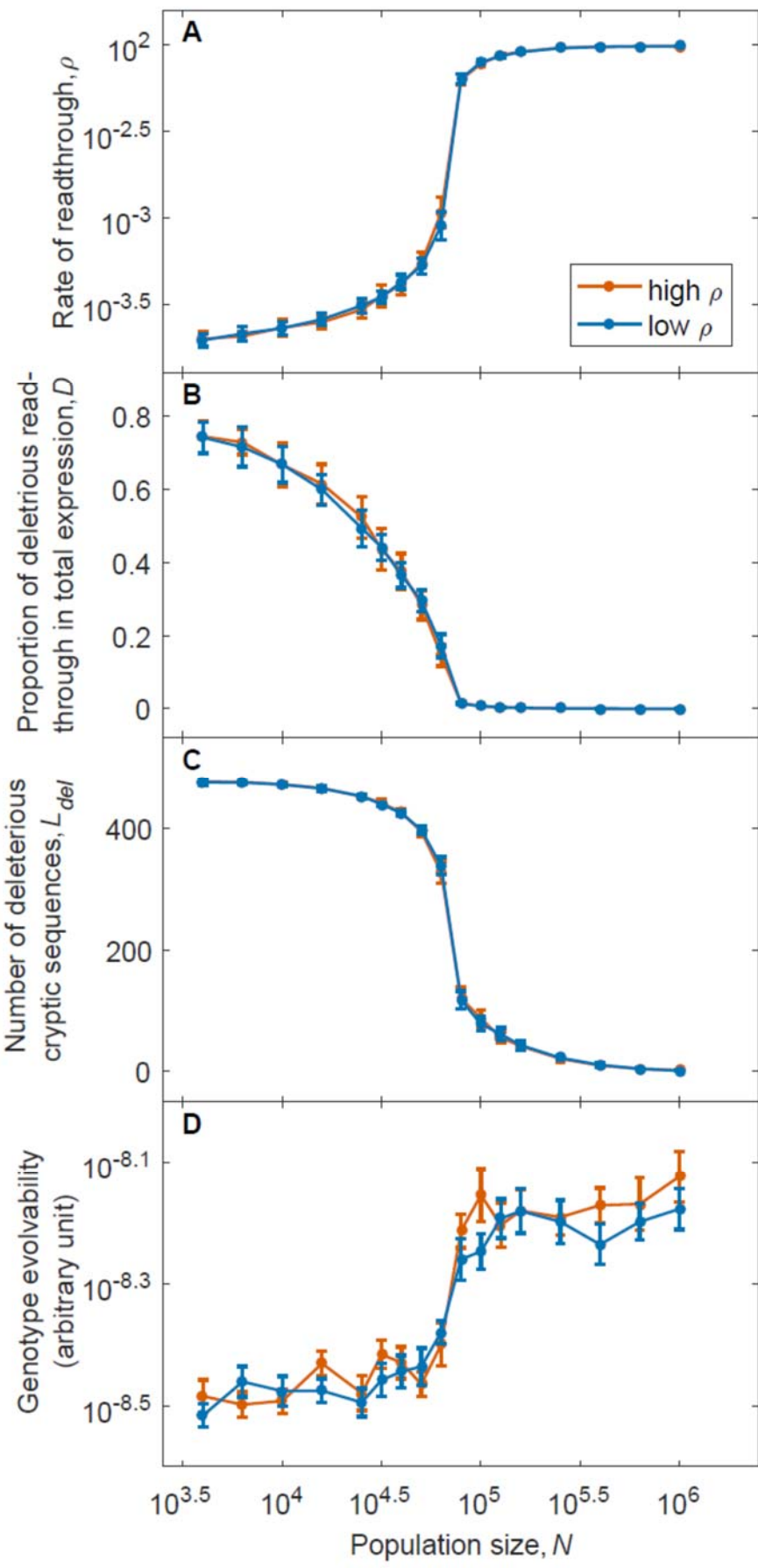


Figure A: At $\sigma_E = 2.25$, the final state of the evolutionary simulation does not depend on the initial conditions. The data shown here is the same as that shown pooled in Fig. 1.

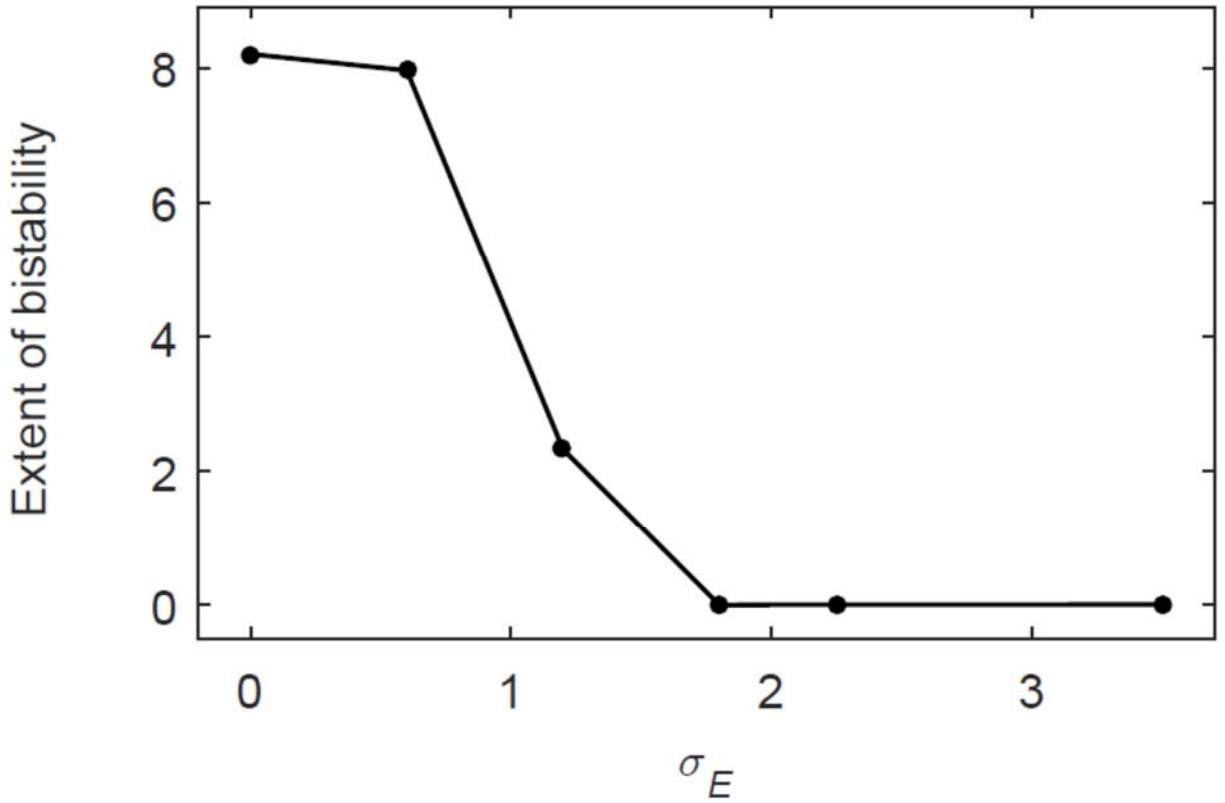


Figure B: The range of population sizes that exhibit significant bistability drops dramatically even for $\sigma_E < 2.25$. We used average values of ρ towards the end of the simulations as a measure of the solution found by each replicate. For each initial condition, we averaged over five replicates (except for $\sigma_E = 0, 2.25$, and 3.5 , where we reused the 20 replicates of Fig. 1), and over each of the values of N between $10^{3.6}$ to 10^6 , with an increment of $10^{0.2}$. The extent of bistability was assessed as $\sum_N (\log_{10} \bar{\rho}_{init_low} - \log_{10} \bar{\rho}_{init_high})^2$. $L = 600$.

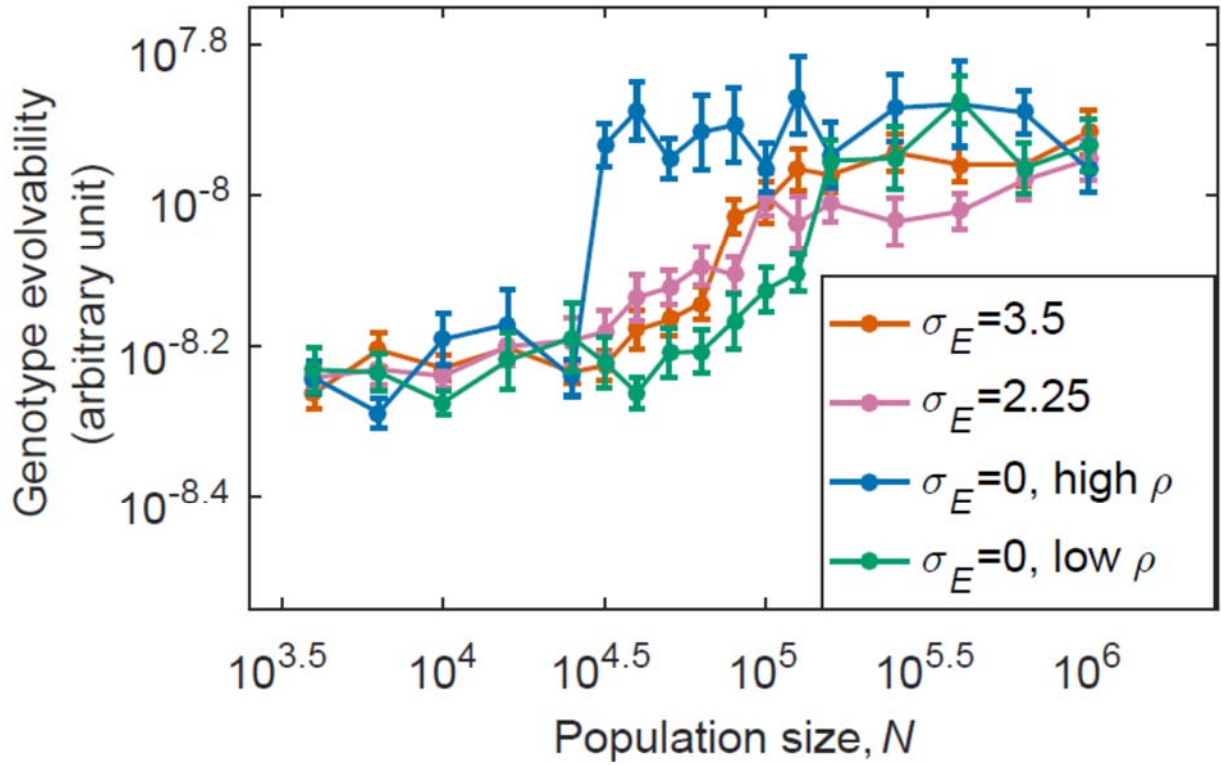


Figure C: The time taken for the trait to approach the new value of x_{opt} behaves similarly to the recovery time of fitness shown in Fig. 1D. The same simulations were used as in Fig. 1. At $\sigma_E = 2.25$ and $\sigma_E = 3.5$, we pooled the results from high- ρ and low- ρ conditions. Evolvability is shown as $\text{mean} \pm \text{SE}$ of the log-transformed values. $L = 600$.

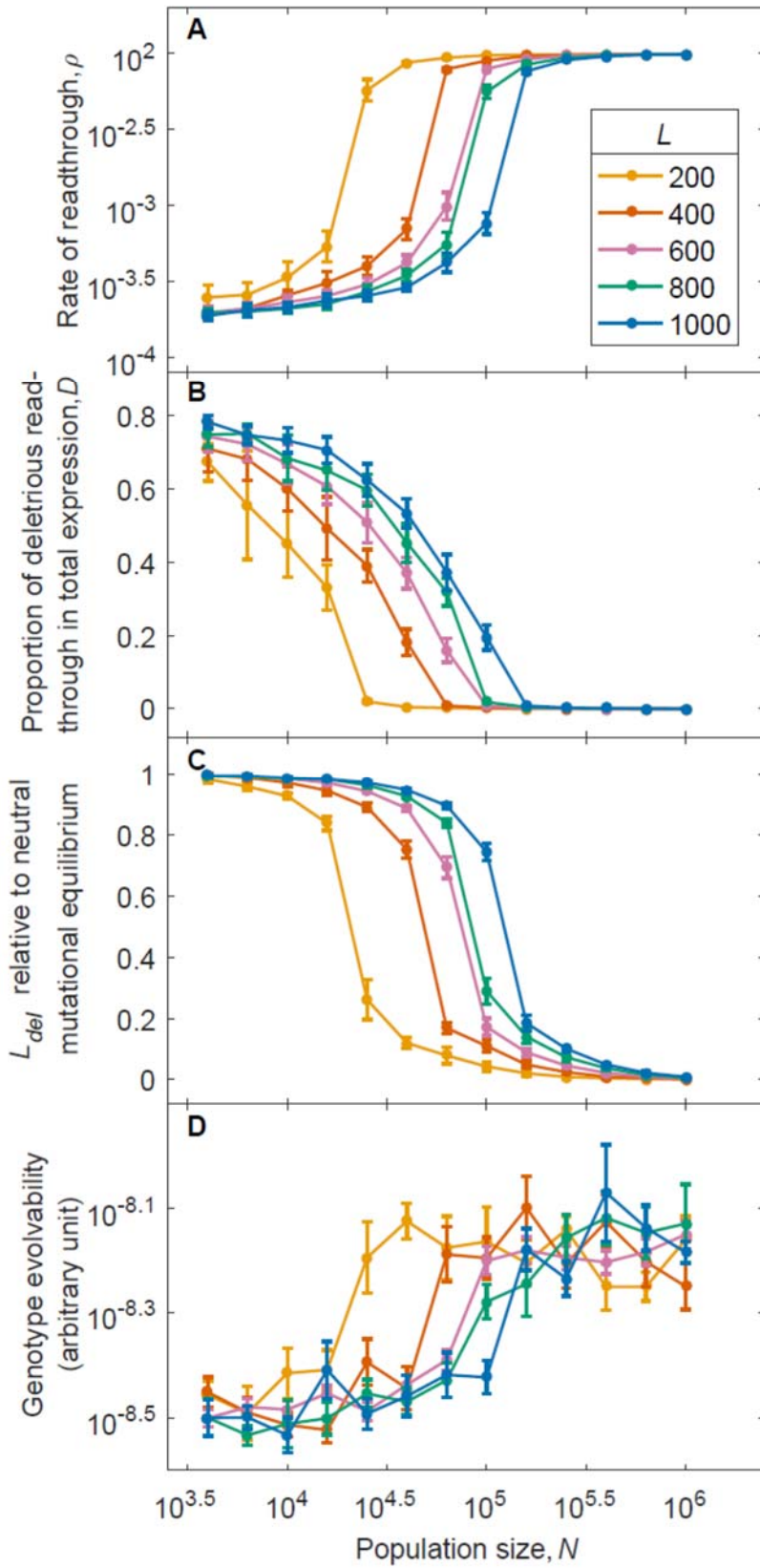


Figure D: Changing the number of loci does not qualitatively change our results.

Quantitatively, fewer loci favor more local solutions. Changing L alters the average contribution of each locus to D . This alters the average strength of selection on each locus, independent of population size. Therefore, the same solutions, characterized by the values of ρ and D , are “shifted” to small values of N as L decreases. While L changed, we held the number of quantitative trait loci constant at 50. For $L = 600$, we reused the results shown in Fig. 1. For other values of L , five replicates were run for each of the two initial conditions. We pooled results from both initial conditions across all values of L . We normalized L_{del} to the neutral mutational equilibrium of $L \times \mu_{del} / (\mu_{del} + \mu_{ben})$. For panels **A** to **C**, data is shown as mean \pm SD. For **D**, data is shown as mean \pm SE. For **A** and **D**, these apply to log-transformed values. $\sigma_E = 2.25$.

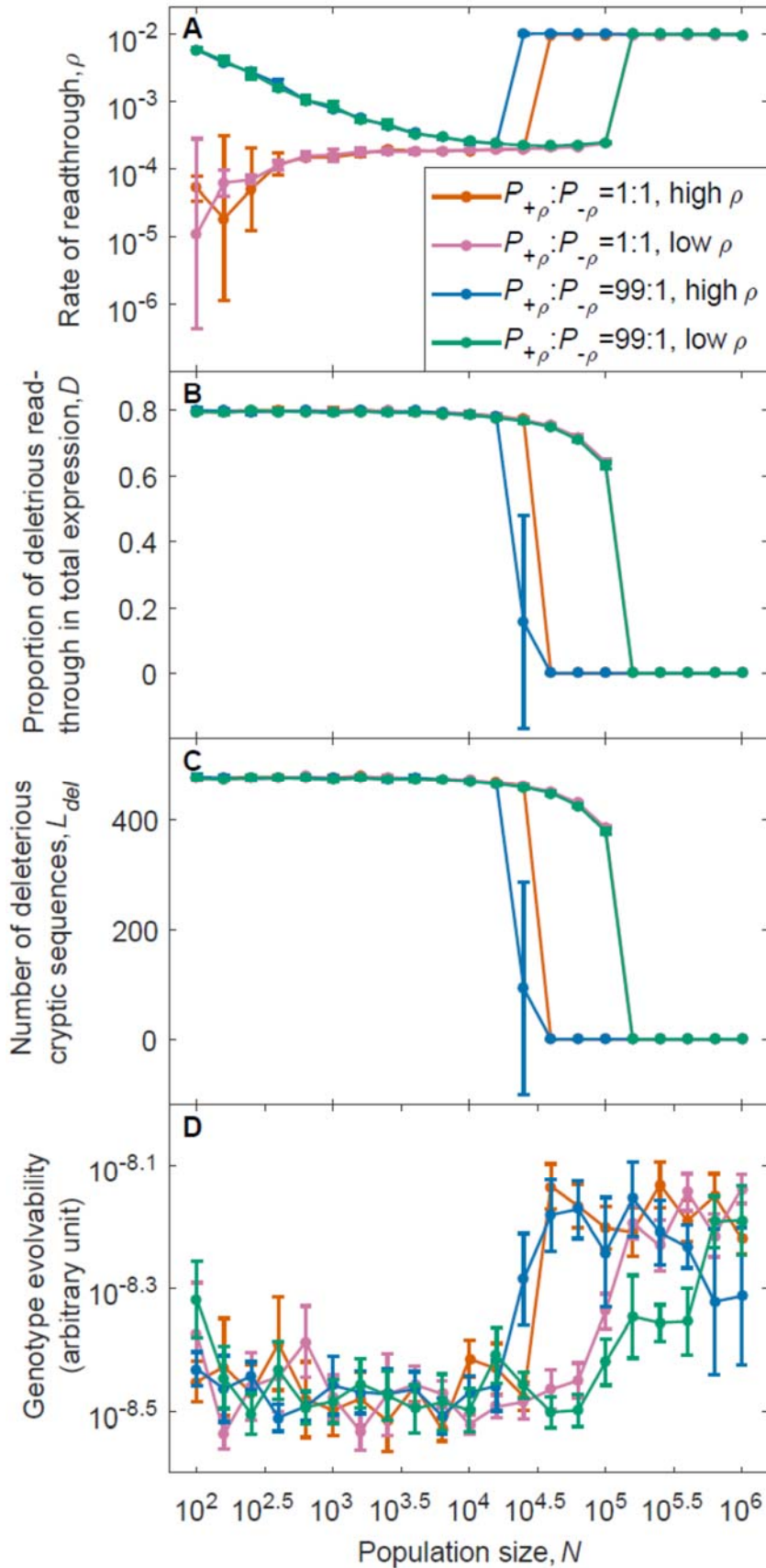


Figure E: Fig. 4 results (that the global solution breaks down in sufficiently small populations) remain true in the absence of variation of expression levels. Data points between $N = 10^{3.6}$ to $N = 10^{6.0}$ and $P_{+\rho}:P_{-\rho} = 1:1$, are reused from Fig. 1; for the others, we performed 5 replicates for each condition. For panels **A** to **C**, data is shown as $\text{mean} \pm \text{SD}$. For **D**, data is shown as $\text{mean} \pm \text{SE}$. For **A** and **D**, these apply to log-transformed values. $L = 600$.

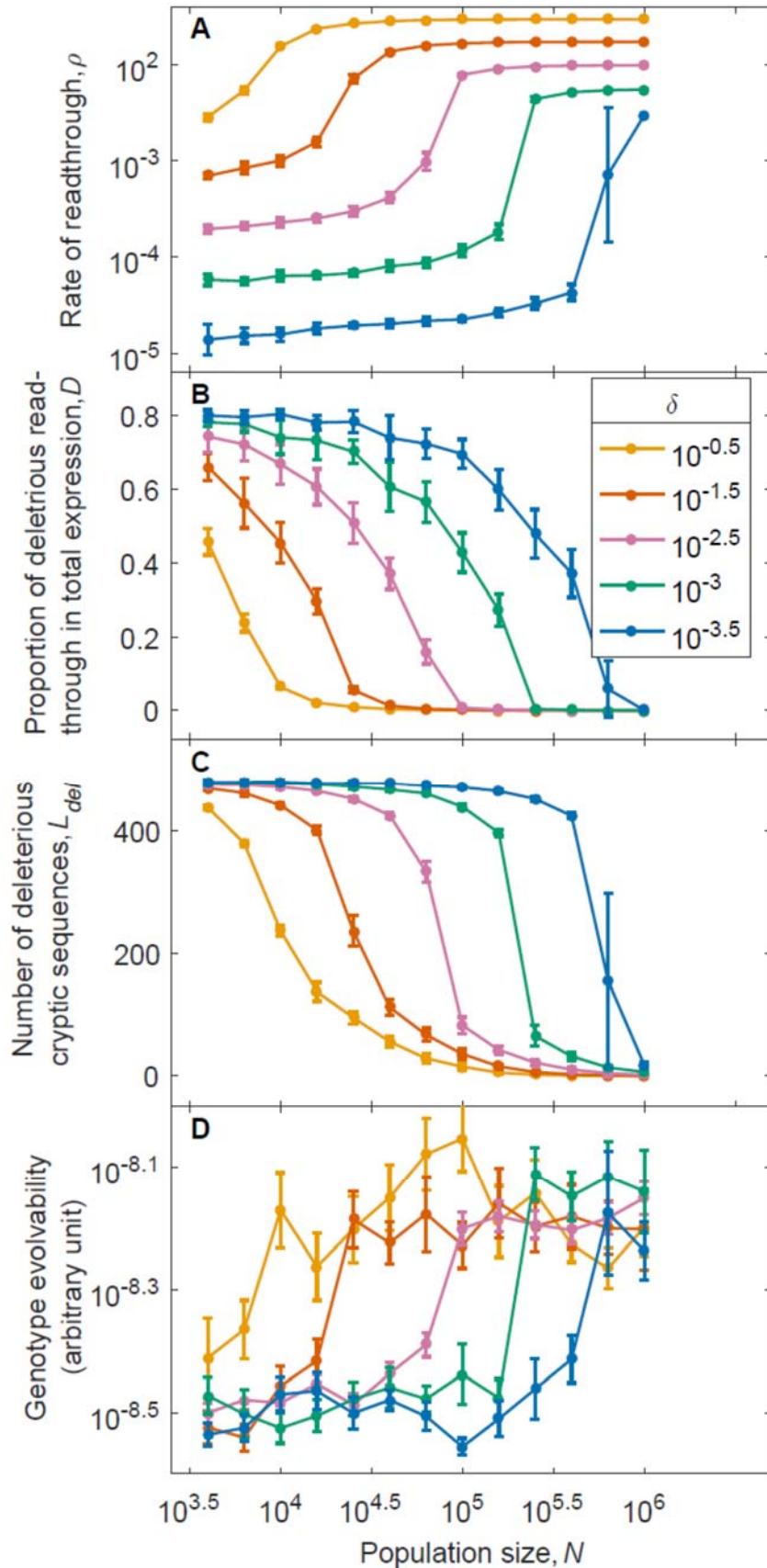


Figure F: Increasing the cost of quality control δ expands global solutions to smaller populations and reduces the differences in error rates as a function of population size. For $\delta = 10^{-2.5}$, we reused the data from Fig. 1; for each of the other values of δ , we ran 5 replicates from the high- ρ initial condition and 5 from the low- ρ initial condition. Each data point represents the pooled results from the two initial conditions. For panels **A** to **C**, data is shown as mean \pm SD. For **D**, data is based on time to fitness recovery and is shown as mean \pm SE. For **A** and **D**, the mean, SD and SE are calculated on log-transformed values. The large error bars at $N = 10^{5.8}$ under $\delta = 10^{-3.5}$ across all panels are due to different initial conditions, which is a sign of bistability. $L = 600$, $\sigma_E = 2.25$.

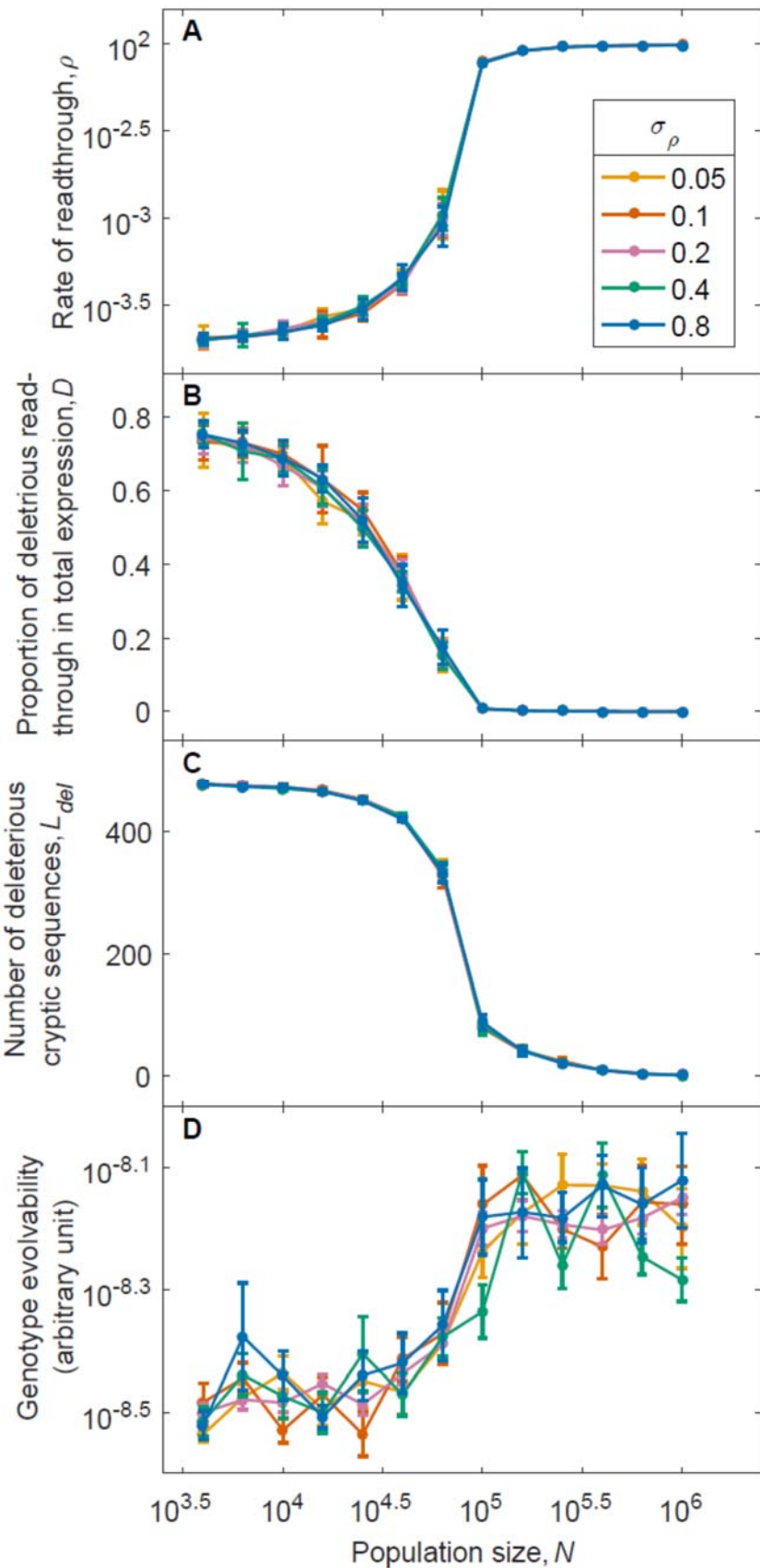


Figure G: The variance in the magnitude of mutations to ρ does not affect a population's solution to error or evolvability. For $\sigma_\rho = 0.2$, we reused the data from Fig. 1; for each of the other values of σ_ρ , we ran 5 replicates from each of the two initial conditions. We pooled results from the two initial conditions for each data point. For panels **A** to **C**, data is shown as mean \pm SD. For **D**, data is based on time to fitness recovery and is shown as mean \pm SE. For **A** and **D**, these apply to log-transformed values. $L = 600$, $\sigma_E = 2.25$.

Table A: Summary of model parameters

Group	Parameter	Biological meaning	Exploration	Parameter values in model ^[1]	Influence on global v. local solutions
Selection for local vs. global solution	σ_E^2	Variance of \log_2 expression among loci	Fig. 1, Fig. S2	5.1 (0-12.3)	Central finding: lower σ_E^2 promotes dichotomy
	c	Cost of misfolding	Fig. S3 ^[2]	20 (7-28 ^[2])	Large c makes ρ smaller, with a slightly larger impact on global solutions, and expands the bistable region to smaller populations.
	δ	Scaling of quality control costs	Fig. S6	$10^{-2.5}$ ($10^{-0.5}$ - $10^{-3.5}$)	Higher cost makes ρ larger, with a larger impact on global solutions, and expands global solutions to smaller populations
	L	Total number of loci	Fig. S4, Fig. S2 ^[2]	600 (200-1000)	Lower L shift the transition between local and global solutions to smaller populations, but maintain the shape of the transition
Mutation bias for local vs. global solution	μ_{del}	Rate of benign-to-deleterious mutations	Fig. 3	$\mu_{del}:\mu_{ben} = 4:1$ (1:1-99:1)	Stronger mutation bias lowers ρ and shifts the transition between local and global solutions to larger populations
	μ_{ben}	Rate of deleterious-to-benign mutations			
	$P_{+\rho} \times \mu_\rho$	Rate of mutations that increase ρ	Fig. 4, Fig. S5	$P_{+\rho}:P_{-\rho} = 1:1$ (1:1-99:1)	Mutation bias prevents extremely small populations from reducing ρ
	$P_{-\rho} \times \mu_\rho$	Rate of mutations that decrease ρ			
	σ_ρ^2	var(mutations to ρ)	Fig. S7	0.04 (2.5×10^{-3} -0.64)	No apparent influence
Relevant only for quantitative effects and evolvability (of peripheral interest to our central findings)	K	Number of quantitative trait loci	Fig. S7 ^[2]	50 (5-50 ^[2])	
	a	Speed that α and β revert to mean	Fig. S10 ^[2]	750 (250-2000 ^[2])	
	μ_{coopt}	Rate of co-option mutations	-	2.56×10^{-9}	
	μ_α	Rate of mutations to α	-	3×10^{-7}	
	μ_β	Rate of mutations to β	-	3×10^{-8}	
	σ_m^2	$\sigma_m^2/K = \text{var}(\text{mutations to } \alpha \text{ and } \beta)$	Fig. S8 ^[2]	0.25 (0.04-1 ^[2])	
	σ_f	Strength of selection on trait	No loss of generality when σ_m^2 only is explored	0.2	

^[1] The numbers outside parentheses are the default values and the numbers inside indicate the parameter range explored.

^[2] Rajon and Masel (2011)

Supplementary References:

Rajon, E., and J. Masel, 2011 The evolution of molecular error rates and the consequences for evolvability. *Proc. Natl. Acad. Sci. U.S.A.* 108: 1082-1087.